

On the Absolute Intensity of Incoherent Scatter Echoes From the Ionosphere

K. L. Bowles, G. R. Ochs, and J. L. Green

Contribution from Central Radio Propagation Laboratory, National Bureau of Standards, Boulder, Colo

(Received January 25, 1962)

New observations have been made of the absolute intensity of incoherent scatter echoes from the ionosphere, at a station near Lima, Peru. In order to analyze these observations properly, the paper begins with a rederivation of the radar equation in its form appropriate to incoherent scatter studies. The result of this derivation is that a correction factor of approximately 2 must be applied to the radar equation in its form generally used in this work. Details given of the observational parameters of the radar system permit precise comparison of the present results with results of other workers. The observations indicate that the average radar cross section *per free electron* is usually close to the theoretically predicted value of one half the classical Thomson cross section. This suggests that the ionosphere is usually in a condition of thermal equilibrium between ions and electrons. Occasionally, particularly at sunrise, the observed cross section is still lower, approximating one quarter of the classical Thomson cross section. This observation would agree with the theoretical predictions of J. A. Fejer [1961] if the electron temperature at sunrise in the *F* region exceeds the ion temperature.

The subject of "incoherent scattering" of radio waves by free electrons, and its application to radar studies of the ionosphere, has received much attention in the three years since Gordon [1958] first proposed its use. Subsequent observations of this effect [Bowles, 1958 and 1961; Pineo et al., 1960 a and b], with echoes actually obtained from the *F* region of the ionosphere, demonstrated that the scatter phenomena are more complicated than the simple Rayleigh scatter from free electrons conjectured by Gordon [1958]. The mathematical theory has now been developed by several groups of workers to explain the scatter which should be observed under a variety of conditions of electron density, magnetic field intensity, radiofrequency of the sounding wave, orientation of the radio path relative to the magnetic lines of force, etc. [Fejer, 1960 a and b, 1961; Salpeter, 1960 a and b, 1961 a and b; Dougherty and Farley, 1960; Renau, 1960; Laaspere, 1960; Hagfors, 1961; Buneman, 1961; Renau et al., 1961; Farley, Dougherty, and Barron, 1961]. Although a variety of theoretical approaches have been used in these papers, the results of the calculations display a remarkable unanimity.

The agreement of the observations with the theoretical predictions has been good enough that there can be no doubt that this particular kind of electronic backscattering is at work. We shall continue in our use of the term "incoherent backscatter" or simply "incoherent scatter." However, it is now clear that the scatter in question should be considered to arise from irregularities in electron density, rather than from randomly distributed free electrons as would be the case with purely incoherent Rayleigh scatter [Rayleigh, 1871]. The spectral

characteristics of the scattered echoes as measured by Pineo et al. [1960b] at MIT, are consistent with the theory for the conditions of their experiment. The vertical profiles obtained by this technique [Bowles, 1961; Pineo et al. 1960b; VanZandt and Bowles, 1960] have been compared with partial profiles of electron density obtained by other methods, notably "true height" analysis of conventional ionograms, and it is certain that at most times the echo power is very nearly—if not indeed exactly—proportional to electron density.

Measurements of the absolute intensity of echoes obtained in Illinois by Bowles [1961] gave a value of the average scattering cross section per free electron in the ionosphere very close to the classical Thomson scattering cross section. Within the range of experimental error the experiments of Pineo et al. [1960] at first appeared to give the same result. Both results appeared to be in disagreement with the theoretical predictions by a factor of approximately 2, inasmuch as the theories all predict an average scattering cross section per free electron of almost exactly *one-half* the Thomson cross section (for the experiments performed at 41 and 440 Mc/s). The factor of 2 disagreement was not taken very seriously in view of the opportunity of error in measurements of this kind.

Recently Pineo has recalculated his early results as well as some obtained later. In a recent publication [Pineo and Briscoe, 1961], he has expressed the belief that the average cross section per free electron, as observed both in his work and that of Bowles [1961] in Illinois, is about one order of magnitude less than the Thomson cross section. Motivated by this, the authors have made a series

of new absolute measurements with a new radar facility near Lima, Peru, and have redeveloped the radar equation in its form applicable to ionospheric backscatter measurements. Our calculations with most of the new results, as well as a recalculation of the older Illinois results, give values of the average scatter cross section per free electron equal to one-half the Thomson cross section (plus or minus about 10 percent). Only at certain hours of the day does the observed cross section depart significantly from this value. An estimate based upon our limited knowledge of the earlier MIT results [Pineo et al., 1960] yields nearly the same value. Three-way correspondence among the authors, Pineo, and J. A. Fejer, has failed to produce agreement on treatment of the observed data. The authors of this paper nevertheless believe their new result, which coincides well with theoretical predictions, to be correct.

The object of the present paper is to present the calculation as we believe it should be done. We give details on all parts of the measurement on which the reader is likely to have some doubt. Those readers with sufficient interest should be able to make the calculation in their own way using the data given.

At the end of the paper, a discussion is given of those observations which do depart significantly from the theoretically predicted value of scatter cross section per free electron. These departures may logically be associated with departures from thermal equilibrium conditions, for example as suggested by Fejer [1961] for the case $T_e/T_i \neq 1$. The writers plan to subject these departures to more thorough experimental investigation for description in a later paper. At present it appears that the value of the scattering cross section per free electron found in our observations is close to the theoretical except during a few hours of the day.

Where $T_e \neq T_i$ spectral measurements offer the opportunity to correct the observed scatter power to its equilibrium value. Thus the existence in the ionosphere of deviations from thermal equilibrium need not compromise seriously the use of incoherent scatter as a measure of the electron density profile. On the other hand the spectrum measurements are difficult to make accurately at all heights simultaneously without the use of an on-line digital computer. We believe therefore that our present observations indicate that thermal equilibrium normally does prevail, and that spectral measurements are not normally required to reduce scatter observations to electron density profiles.

1. Derivation of the Radar Equation

The form of the radar equation applicable to backscatter measurements can be derived most simply in several functional stages related to the scattering process.

(Power received) = (flux incident upon the antenna) \times (effective aperture of the antenna) \times (loss factor),

(flux incident upon the antenna) = (flux incident upon scattering volume) \times (fraction of incident power reradiated by unit volume) \times (total scattering volume) \times (range attenuation).

Several basic assumptions will be used throughout.

(a) The scattering volume is small enough that all parts of the volume may be assumed to lie at the same range from the radar station.

(b) The radar is monostatic—the same antenna serves both for transmitting and for receiving.

(c) The range to the scattering volume is large compared to the largest dimension of the radar antenna.

The following symbols will be used. Units are rationalized MKS.

P_t = Peak power during the transmitted pulse, measured at the terminals of the transmitter. (See text for precise definition related to pulse shape.)

P_r = Power received—power at the receiver terminals available to a resistive load having the characteristic impedance of the antenna transmission line Z_0 (resistive).

P_{inc} = Power, in the scattered signal, passing through an area equal to the physical aperture area of the antenna.

τ = Duration of the transmitted pulse.

A = Physical aperture area of the antenna.

$A(\theta, \phi)$ = Effective aperture of the antenna at an angle θ from the main axis of the principal lobe, and at azimuth angle ϕ .

$G(\theta, \phi)$ = Gain of the antenna over a lossless isotropic radiator at angles θ and ϕ .

a, b = Dimensions of the antenna aperture defined in the text.

λ = Radio wavelength in free space. (In our experiments $\lambda = 6m$).

λ_d = Debye shielding distance.

R = Range to the scattering volume. $R \gg a$ or b .

N = Density of free electrons per cubic meter.

σ_e = The radar cross section of a single free electron. (See text for definition.)

σ_m = The radar cross section of the scattering volume *per* free electron.

σ = The radar cross section of the scattering volume per cubic meter.

η_r = Efficiency of the antenna and transmission lines considering resistive losses alone.

η_A = Aperture efficiency of the antenna considering the power distribution in the feed system as it affects the principal lobe.

η_s = Aperture efficiency of the antenna considering the power distribution in the feed system as it affects the sidelobes.

- $\Phi_s(\theta, \phi)$ = Power flux density incident at the scattering volume from the transmitter at angle (θ, ϕ) .
- $\Phi_A(\theta, \phi)$ = Power flux per steradian scattered in the direction of the antenna from a volume of unit area and depth $c\tau/2$ at angle (θ, ϕ) .
- c = Velocity of light in free space = 2.998×10^8 m/sec.

1.1. Flux Incident Upon the Scattering Volume

If the transmitted power were radiated by an antenna with an isotropic gain pattern, the power would be uniformly distributed over the surface of a sphere at range R , and the incident flux density would be

$$\frac{P_t \eta_r}{4\pi R^2} \text{ watts per square meter.}$$

Allowing the antenna to have a gain pattern, the flux density at range R becomes a function of direction

$$\Phi_s(\theta, \phi) = \frac{P_t \eta_r G(\theta, \phi)}{4\pi R^2} \text{ watts per square meter.}$$

1.2. Fraction of Incident Power Reradiated by a Unit Volume

There are several conventions for the definition of radar cross section σ . We shall use the convention that the scattering center whose radar cross section is σ , is considered equivalent to a center which reradiates isotropically an amount of power equal to the power passing through an area σ , located at range R from the radar transmitter. By "equivalent" we mean that such an ideal isotropic scatterer would give rise to the flux actually observed at the receiving antenna. An equally acceptable convention, which we shall not use, is that the scattering center whose radar cross section is σ' , reradiates per steradian of solid angle in the direction of the receiver an amount of power equal to the power passing through an area σ' located at range R . Evidently if this latter scattering center were to reradiate isotropically the total power reradiated would be $4\pi\sigma'\Phi_s$. This same power on the first convention would be $\sigma\Phi_s$, so that $\sigma = 4\pi\sigma'$.

The classical scattering cross section of the free electron, i.e., the Thomson scattering cross section, is well known and may be found in most texts on modern physics or X-ray diffraction. We quote Richtmyer, Kennard, and Lauritsen [1955]: The quantity $(8\pi e^4)/(3m^2 c^4)$, "which will be denoted by σ_e , is called the classical scattering cross section or coefficient for a free electron. As much of the incident energy is scattered as passes through an area of magnitude σ_e drawn perpendicular to the incident beam. Inserting $e = 4.803 \times 10^{-10}$, $m = 0.9109 \times 10^{-27}$, $c = 2.998 \times 10^{10}$, we find $\sigma_e = 6.65 \times 10^{-25} \text{ cm}^2$." (Note use by Richtmyer et al. [1955] of CGS units in con-

trast to the MKS units in our calculations, also our slight change of their notation.) In MKS units $\sigma_e = 6.65 \times 10^{-29} \text{ m}^2$.

Now the free electron scatters radio energy not isotropically but approximately as a short dipole, i.e., a Hertzian dipole. Consequently it scatters energy best in the plane perpendicular to the orientation of the electric field in the incident wave, and not at all in the direction parallel to that orientation. Within the preferred plane the gain of the short dipole is $G = 1.5$ [Lovell and Clegg, 1952]. Thus the free electron scatters power back to the radar with a cross section σ_e equivalent to an isotropic scatterer whose cross section is $\sigma = 1.5 \times 6.65 \times 10^{-29} = 9.97 \times 10^{-29} \text{ m}^2$. This would be the value of σ_m , the observed scattering cross section per free electron of the ionospheric plasma, if the electrons were to scatter truly incoherently, i.e., in random phase. (Phase of the contribution from each free electron is considered statistically independent of the phase of the contribution from every other free electron.) According to the theoretical predictions already referenced, if the radio wavelength is considerably larger than the Debye shielding distance, λ_D of the plasma in question, the value of σ_m should be $\frac{1}{2}$ this classical value.

$$\sigma_m = 4.99 \times 10^{-29} \text{ m}^2. \quad (1)$$

The conditions for this to hold, $\lambda_D \ll \lambda$, obtain in the F' region of the ionosphere for both the NBS and MIT experiments, since $\lambda_D \approx 0.002$ m and λ is of the order of 1 m.

Our unit of volume is the cubic meter, hence the observed scattering cross section per unit volume should be

$$\sigma = N \sigma_m \frac{(\text{meter})^2}{(\text{meter})^3}. \quad (2)$$

1.3. Total Scattering Volume

For simplicity we assume that the transmitted pulse is rectangular, P_t being constant during the period of the pulse τ , and zero at all other times. Both the present series of experiments, as well as that of Bowles [1961], have in fact employed approximately rectangular pulses, and our understanding is that Pineo et al. have done the same. In any event, since the scattered power contributions from various parts of the pulse are assumed to add linearly, τ represents the duration of a rectangular pulse containing the same energy as the actual transmitted pulse for purposes of calculating the absolute scattered power. The depth of the scattering volume is therefore $c\tau/2$. The element of area at distance R is $R^2 \sin \theta d\theta d\phi$. Hence the scattering volume within a given incremental solid angle is

$$\frac{c\tau R^2 \sin \theta d\theta d\phi}{2}.$$

1.4. Range Attenuation

The scattered power, according to our convention, is distributed evenly over the area of a sphere of

radius R , i.e., over an area $4\pi R^2$. Our "range attenuation" factor is therefore

$$\frac{1}{4\pi R^2} m^{-2}.$$

1.5. Flux Incident Upon the Antenna

Combining the above factors we obtain the scattered flux per steradian incident upon the antenna arising from an elemental volume at angle (θ, ϕ)

$$\begin{aligned} \Phi_A(\theta, \phi) d\theta d\phi &= \frac{P_t \eta_r G(\theta, \phi)}{4\pi R^2} \sigma \frac{c\tau R^2 \sin \theta d\theta d\phi}{2} \frac{1}{4\pi R^2} \\ &= \frac{P_t \eta_r G(\theta, \phi) \sigma c\tau \sin \theta d\theta d\phi}{32\pi^2 R^2}. \end{aligned} \quad (3)$$

1.6. Effective Aperture

Readers are referred to the books by Silver [1949], and by Schelkunoff and Friis [1952], for discussions of the concept of antenna aperture. Note that we use the term $G(\theta, \phi)$ to mean the same as "directivity," of the main lobe. Resistive losses are accounted for separately through use of the efficiency factor η_r .

If an antenna having a physical area or aperture A , collects all of the power incident upon its aperture along its main axis, it displays a "gain"

$$G = \frac{4\pi A}{\lambda^2}$$

in its axial direction. The antenna collects G times as much power from a source in that direction as does an isotropic antenna. On transmitting it radiates a flux in the axial direction G times as great as does an isotropic antenna radiating the same power. The concept of gain relates to the increase of antenna response in some particular direction relative to a device which distributes the radiated energy uniformly in all directions. Outside its main beam, the gain of a radar antenna is much less than unity on the average, although occasional sidelobes may exceed unity gain.

In order to complete our calculation we assume that $G(\theta, \phi)$ is known. Later in the discussion, $G(\theta, \phi)$ will be related to the physical apertures, A , of various real antennas. Then the effective aperture in any direction (θ, ϕ) of an antenna free of resistive losses is

$$A(\theta, \phi) = \frac{G(\theta, \phi) \lambda^2}{4\pi}. \quad (4)$$

1.7. Loss Factor

Those resistive losses which affect equally all parts of the current distribution across the antenna aperture may be considered as equivalent to losses in the antenna transmission line system, and do not affect the directivity function $G(\theta, \phi)$. The factor

η_r is used to account for the one way losses of this nature either when transmitting or when receiving. Those resistive losses which affect the various parts of the aperture current distribution unequally modify $G(\theta, \phi)$ and must be considered to be included in that function for purposes of our calculation.

1.8. Power Received

The power received, P_r , must be related to the flux of energy crossing the antenna aperture in order to meet our requirements. If the antenna is loaded with a resistive impedance equal to its characteristic impedance, maximum transfer of power takes place from the power crossing the antenna aperture into the load impedance. This is the power available to a resistive load, and is equal to the power crossing the antenna effective aperture or collecting aperture. Representation of the antenna as a Thevenin equivalent generator sometimes is used incorrectly as an argument that one half of the incident power is scattered, or reradiated, by the antenna. A large antenna, such as one useful for incoherent scatter studies, is more correctly thought of as an impedance matching device permitting all of the power incident upon the collecting aperture to be dissipated in the load [Silver, 1949].

Just as a portion of the power $(1 - \eta_r)P_t$ leaving the transmitter terminals is absorbed resistively, so a like portion of the power incident upon the effective antenna aperture is dissipated and is not available at the receiver terminals. Hence we have

$$P_r(\theta, \phi) d\theta d\phi = \Phi_A(\theta, \phi) A(\theta, \phi) \eta_r d\theta d\phi.$$

$$P_r = \eta_r \int_{\theta} \int_{\phi} \Phi_A(\theta, \phi) A(\theta, \phi) d\theta d\phi. \quad (5)$$

Combining eqs (3), (4), and (5)

$$P_r = \frac{P_t \eta_r^2 \sigma c\tau \lambda^2}{128\pi^3 R^2} \int_{\theta} \int_{\phi} G^2(\theta, \phi) \sin \theta d\theta d\phi. \quad (6)$$

1.9. Approximate Expression for P_r

It is customary to approximate the integral in eq (6), by representing the antenna gain pattern $G(\theta, \phi)$ as uniform within a rectangular solid angle bounded by the half power limits of the true gain pattern along its two principal axes. The approximation represents the gain as zero outside these limits. The value of $G(\theta, \phi)$ within these limits is taken to be equal to the gain of the true beam along its main axis.

$$G = \frac{4\pi A_{\text{eff}}}{\lambda^2} \quad (7)$$

A_{eff} is here defined as the effective collecting aperture of the antenna, in lieu of $A(\theta, \phi)$. $A_{\text{eff}} = A$, the physical aperture, for an antenna having a uniformly distributed feed system. Since A_{eff} is directly related to the directivity it represents, in the case of an antenna with a tapered feed distribution, the area

of a uniformly fed aperture giving the same beamwidths and gain to the main lobe. In this case we define the aperture efficiency $\eta_A = A_{\text{eff}}/A$.

Now it is also customary to approximate the solid angle occupied by the main beam within its half power limits as equal to λ^2/A_{eff} . This follows from the approximation for a uniform linear array of length a , that the beamwidth in a plane containing the array is (λ/a) . Thus for a uniformly illuminated lossless rectangular aperture ($\eta_A=1$) of dimensions a , and b , it is natural to write

$$\frac{\lambda}{a} \frac{\lambda}{b} = \frac{\lambda^2}{A} = \frac{\lambda^2}{A_{\text{eff}}}$$

We may now approximate the integral of eq (6):

$$\int_{\theta} \int_{\phi} G^2(\theta, \phi) d\theta d\phi \approx \left[\frac{4\pi A_{\text{eff}}}{\lambda^2} \right]^2 \int_{\theta=0}^{\theta_{\frac{1}{2}}} \int_{\phi=0}^{2\pi} \sin \theta d\theta d\phi \quad (8)$$

but

$$\int_{\theta} \int_{\phi} \sin \theta d\theta d\phi \approx \frac{\lambda^2}{A_{\text{eff}}}$$

the solid angle occupied by the beam, hence

$$\int_{\theta} \int_{\phi} G^2(\theta, \phi) \sin \theta d\theta d\phi \approx \left[\frac{4\pi A_{\text{eff}}}{\lambda^2} \right]^2 \frac{\lambda^2}{A_{\text{eff}}} = \frac{16\pi^2 A_{\text{eff}}}{\lambda^2} \quad (9)$$

Combining eqs (6) and (9) we obtain

$$P_r \approx \frac{P_t \eta_r^2 \sigma c \tau A_{\text{eff}}}{8\pi R^2} \quad (10)$$

1.10. Role of Sidelobes

Thus far we have made no mention of the role of sidelobes in the antenna response pattern. Since power radiated into sidelobes is not available to the main beam, their presence represents a reduction of aperture efficiency. In the integral eq (6) for P_r , this reduction is automatically taken into account, since we assume knowledge of $G(\theta, \phi)$ at all angles. No accounting for sidelobes has been made in the approximate expression (10) since A_{eff} is determined only on the basis of the directive characteristics of the main lobe. Thus while η_A represents an aperture efficiency, it applies only to the directivity of the main lobe.

Power radiated on transmitting into the sidelobes leaves a fraction η_s of the transmitted power for the main beam. Hence in eq (10) we must replace P_t with the expression $P_t \eta_s$. Likewise on reception the gain of the antenna in the main lobe is reduced, so that A_{eff} must be replaced by $\eta_s A_{\text{eff}}$. This leads to

$$P_r = \frac{P_t A \sigma c \tau \eta_r^2 \eta_s^2 \eta_A}{8\pi R^2} \quad (11)$$

which, except for differences of notation, is the approximate form of the radar equation used thus far by all workers in incoherent scatter.

1.11. Sources of Error in the Approximate Equation for P_r

We recall that the development of eq (11) was based on equivalence of any antenna to a uniformly illuminated, lossless, rectangular aperture of dimensions a and b , and physical aperture $Aa=b$. The power gain of such an array is given by the equation [Schelkunoff and Friis, 1949] (in form correct for our notation)

$$G(\theta, \phi) = \frac{4\pi A}{\lambda^2} \frac{\sin^2 \left(\frac{\pi a}{\lambda} \sin \theta \cos \phi \right) \sin^2 \left(\frac{\pi b}{\lambda} \sin \theta \sin \phi \right)}{\left(\frac{\pi a}{\lambda} \sin \theta \cos \phi \right)^2 \left(\frac{\pi b}{\lambda} \sin \theta \sin \phi \right)^2} \quad (12)$$

where $\phi=0$ is chosen along the axis parallel to the side of dimension a .

In obtaining eq (11) the gain pattern of eq (12) was approximated as uniform within a rectangular solid angle the sides of which were λ/a and λ/b . In the special case where $a=b$, precise calculation easily reveals that a better approximation, having the same integral of the gain throughout the main lobe, would be a circular pattern of angular diameter $0.9 \lambda/a$. In eq (9) the quantity λ^2/A_{eff} , representing the equivalent solid angle occupied by the beam should therefore be replaced by $0.81 \pi \lambda^2 / 4A = 0.63 \lambda^2 / A$. While the correct approximation in the case of $a \neq b$ would not be a circular pattern, the equivalent solid angle would still be given by this expression. The factor 0.63 in this expression may be considered equivalent to the sidelobe efficiency factor η_s . Employing this in eq (11) we obtain a better approximate expression for P_r in the case of a uniformly illuminated rectangular aperture.

$$P_r = \frac{0.4 P_t A \sigma c \tau \eta_r^2}{8\pi R^2} \quad (13)$$

An alternate method of arriving approximately at this same result is to recall that in eq (6), the correct eq for P_r in its integral form, the gain appears as $G^2(\theta, \phi)$. In the approximation it would therefore be better to represent the antenna beam as circular and having the width appropriate to the angular deviation where G^2 falls to one half its maximum. From eq (12) this width is found to be $0.67 \lambda/a$ for the square aperture. The equivalent solid angle therefore becomes $0.35 \lambda^2 / A$.

1.12. Precise Expression for P_r

We have completed the integral of eq (6) for two idealized antenna aperture distributions; a uniformly illuminated square aperture, and a circular aperture with a Gaussian taper. These two probably represent the extremes likely to be encountered in practical antennas for incoherent scatter work.

In the case of the square aperture we have approximated the form of the eq (12) with a circular pattern the profile of which is the same as the profile of eq (12) along one of its principal axes. We estimate that the error produced by making this approxima-

tion is on the order of 1 or 2 percent. The results of the integration are:

$$P_r = 0.43 \frac{P_t A \sigma c \tau \eta_r^2}{8\pi R^2}$$

for uniformly illuminated square aperture (14)

$$P_r = 0.50 \frac{P_t A_{\text{eff}} \sigma c \tau \eta_r^2}{8\pi R^2}$$

for circular aperture with a Gaussian taper (15)
where we define

$$G(\theta) = G_0 \exp \left\{ -\frac{\theta^2}{\alpha^2} \right\} \quad \theta \ll 1$$

$$G_0 = \frac{4\pi A_{\text{eff}}}{\lambda^2} \quad \text{and} \quad A_{\text{eff}} = \frac{\lambda^2}{\pi \alpha^2}$$

2. Experimental Technique

All of the new experimental results reported herein have been obtained at the new radar observatory facility near Lima, Peru, operated jointly by the National Bureau of Standards and the Instituto Geofísico del Perú, latitude 11°56' south, longitude 76°52' west. In table 1 these new results, based upon measurements at the height of maximum electron density in the F2 layer, are compared with a new calculation of the Illinois result of Bowles [1961], and an approximate calculation based upon information available to us from MIT [Pineo et al., 1960 and 1961]. In the latter two cases we shall not dwell upon details of experimental technique.

For convenience we rewrite eq (14) to yield σ_m explicitly (also accounting for η_s and η_A)

$$\sigma_m = \frac{8\pi R^2 P_r}{0.43 P_t A N c \tau \eta_r^2 \eta_s^2 \eta_A} \quad (16)$$

In the text that follows we treat each of the quantities in this equation in terms of the accuracy to which it is known. The use of eq (14), with the correction factor 0.43, is justified since our antenna is a close approximation to a uniformly illuminated aperture.

2.1. A—Antenna Physical Aperture

This aperture was square for measurements listed in table 1 where $A = 2.1 \times 10^4 \text{ m}^2$. Those measurements where $A = 4.3 \times 10^4 \text{ m}^2$, used two adjacent squares of equal size. Some slight difference in the 0.43 correction factor may be necessary for the larger rectangular array. This is not likely to be more than about 1 percent and we shall ignore the difference.

The antenna is an array of half-wave dipoles located 0.3 wavelength above a reflecting screen of poultry netting. Independent feeds are used for the two orthogonal polarizations. These feeds are coupled at the main feed point through a conventional coaxial hybrid coupler. Through a quarter-wavelength difference in transmission line length the array radiates circular polarization. The received signal is taken from the orthogonal tap of the hybrid coupler. We have checked the antenna for pureness of polarization by using the incoherent

TABLE 1. Details on cross section measurements

Date (1961)	Local time	Receiver bandwidth	Pulse duration	P_t	$f_o F_2$	N_{max}	$h_{\text{max}} F_2$	$I_d(h_{\text{max}})$	$P_r(h_{\text{max}})$	A	σ_m
		kc/s	μsec	kw	Mc/s	10^{11} m^{-3}	km	ma	Watts $\times 10^{-16}$	$\text{m}^2 \times 10^4$	10^{-29} m^2
15 July	1633	2.54	500	136	8.0	7.93	410	45	4.57	2.15	3.28
16 July	1437	2.54	500	131	7.2	6.43	400	45	4.57	2.15	3.99
16 July	1609	2.54	500	131	8.0	7.93	400	54	5.49	2.15	3.89
12 August	1544	2.54	500	124	9.6	11.4	380	144	14.6	4.3	3.43
12 August	1730	2.54	500	125	9.4	11.0	370	167	17.0	4.3	3.91
13 August	0555	2.54	500	125	4.5	2.50	290	45.7	4.65	4.3	2.89
13 August	0657	2.54	500	125	6.5	5.23	295	73.6	7.48	4.3	2.31
13 August	0919	2.54	500	125	7.8	7.55	375	92.0	9.35	4.3	3.23
13 August	0957	3.65	300	133	7.5	6.98	375	37.2	5.43	4.3	3.16
13 August	1258	3.65	500	125	8.3	8.54	390	79.7	11.6	4.3	3.84
15 August	0022	3.65	500	125	8.0	7.93	280	120	17.5	4.3	3.20
15 August	0052	2.54	500	125	7.7	7.35	290	149	15.1	4.3	3.20
15 August	0732	3.65	500	124	7.9	7.73	300	77.3	11.3	4.3	2.43
15 August	0747	2.54	500	124	8.3	8.55	310	128	13.0	4.3	2.70
15 August	0813	3.65	500	124	8.7	9.40	295	87.5	12.8	4.3	2.19
15 August	0834	2.54	500	124	9.0	10.05	350	145	14.7	4.3	3.32
15 August	0902	3.65	500	124	9.0	10.05	370	94	13.7	4.3	3.45
15 August	1106	2.54	500	124	8.1	8.14	390	115	11.7	4.3	4.06
15 August	1136	3.65	500	124	8.3	8.55	410	69.6	10.2	4.3	3.61
19 August	0709	5.64	500	124	7.0	6.08	280	50.6	11.4	4.3	2.73
19 August	0732	5.64	500	124	8.1	8.14	300	64.0	14.4	4.3	2.95
19 August	0751	2.54	500	124	8.8	9.60	320 (est)	152	15.4	4.3	3.05
19 August	0820	5.64	500	124	9.3	10.7	325	92.6	20.9	4.3	3.83
**											
24 Feb. 1959	1430	9.6	120	1000	12.6	19.7	360	10	3.8	1.6	5.7

8 Feb. 1960	1430	11	500	2500	13.2	21.6	360	3.8	1.7	0.052	3.6

**NBS=Long Branch, Ill. [Bowles 1961], 3 db correction made for randomization of polarization by Faraday effect, $\eta_r \eta_s = 0.30$.

***MIT, Millstone Hill, Pineo et al. [1960a and b] values given are estimated from private communication with V. C. Pineo [1960, 1961]—

estimated antenna temperature 1100 °K.

estimated signal/noise at $h_{\text{max}} = 1$.

estimated $\eta_r = 0.63$, $\eta_r \eta_A = 0.35$, we assume $\eta_A = 0.6$, therefore $\eta_s = 0.58$.

scatter echo itself. When the received echo approximated 10 times the background noise power on the desired polarization, the opposite polarization showed no evidence of an echo, despite the use of 17 db of signal-noise improvement by averaging the receiver output. This result indicates no significant loss in the system due to cross polarization coupling.

A, the physical aperture of our array, has been measured to an accuracy better than 1 percent.

2.2. η_A —Aperture Efficiency of the Main Lobe

As in the case of the Illinois array [Bowles, 1961], we have measured the shape of the pattern using a radio star, IAU 09S1A [Mills, Slee, and Hill, 1958]. Both the main lobe and one of the primary sidelobes of the beam have been identified with this star, and found to have the relative intensity and angular width predicted for a uniformly illuminated aperture. The major axes of the antenna cross section are oriented at 45° from the magnetic North-South. It is for this reason that we expect and observe only one primary sidelobe of the beam.

Inasmuch as the directional properties of the principal lobe, and primary sidelobe, agree well with the properties of an ideal uniformly illuminated aperture, we set $\eta_A=1$.

2.3. $\eta_r\eta_s$ —Aperture Efficiency Due to Sidelobe and Resistive Losses

The majority of the feed system of the antenna is accomplished with 6 in. coaxial aluminum transmission line. The losses in this line have been estimated theoretically and also measured and they amount to about 15 percent. Additional resistive losses in the small modular sections of the array, as well as in the dipoles themselves can only be estimated. Since the feedpoint of each modular section is matched individually, some small variation in feed of the various sections of the array is expected. The power represented by the fluctuations in this feed intensity will mainly appear as sidelobe energy and hence will reduce the gain in the main lobe.

In view of the difficulties of making an accurate overall estimate of the efficiency factors η_r and η_s we have chosen to depend upon direct measurement of the axial gain of the main lobe. This was accomplished by using the moon as a target, and measuring only the intensity of the first few hundred microseconds of the echo. By restricting the measurement to this region, the moon appears as a diffuse target whose angular width is nevertheless an order of magnitude smaller than our beam width. Absolute gain was measured by comparing the received signal on a reference antenna with that of the big array. The reference antenna was a square array of four dipoles situated 0.2 wavelength above a reflecting sheet of poultry netting. The dipoles were spaced 3 wavelengths apart in order to make mutual coupling effects negligible. Due to lunar libration, the echo faded during the transit of the beam, with a fading period of several seconds duration. The individual fades displayed a high degree of correla-

tion on the two antennas. Samples used to calculate the antenna gain were obtained from the maxima of the fades, since at these times the wave fronts approaching the antenna field must have been most nearly plane. Both antennas were operated in circular polarization. Circular polarization was accomplished in the reference antenna by situating individual linear dipoles at the corners of two 3 wavelength squares, the square of one linear polarization being rotated 45° relative to the square of the other. Neither reference antenna nor the array displayed any significant echo in the opposite circularly polarized mode.

Daytime passes of radio star IAU09S1A have uniformly displayed amplitude scintillations. The scintillations amount to a random modulation of about ± 20 percent over the ideal trace of the star through the antenna beam. The typical scintillation period amounts to several seconds. Angular scintillation during the day appears to be small compared with the beamwidth, being confined to the spread of the trace one would expect from the random modulation of the signal. A comparison of detailed fading on the two halves of the big array revealed almost perfect correlation in detail. The scintillation may therefore be expected to have an instantaneous effect on the gain of the array, for targets beyond the scintillating layer of the ionosphere. For averages of echo level over several minutes, as all of our incoherent scatter measurements have been, the scintillations should have a negligible effect on the system sensitivity.

The measurements made during the moon pass displayed a variation about the average angular variation of gain of about ± 20 percent. This variation presumably originated with the same phenomenon responsible for the star scintillation. An average curve through the apparent gain variations during the lunar transit was estimated visually. Any variation of the estimate by more than ± 3 percent resulted in a curve obviously outside the range of error. A more sophisticated method of averaging was not used since the moon did not pass through the exact center of the main beam. Instead the beam was deflected 1.73° from its central axis by phasing of the individual modular sections of the array (each module is a square six wavelengths on a side). The result was that the exact mathematical form of the expected gain variation with time during the moon pass was in question by ± 2 or 3 percent. A later attempt to measure the gain of the antenna, during a pass of the moon precisely through the central axis of the beam, failed due to the nighttime scintillation effects of equatorial spread- F . The half power width of the main beam was spread to approximately 5° during this period. A separate report on this observation is being prepared.

In coming to the final result of this measurement we have assumed that the efficiency of the individual reference dipoles amounted to about 95 percent. The 5 percent losses are meant to account for losses in the RG8/U balun connection, and resistive losses

in the quarter wave matching transformer and the dipole itself. Both dipole and transformer were constructed of 1 in. diam aluminum tubing.

Separate but identical receivers were used to compare the echo intensity on the reference antenna and on the array. Recording was accomplished on a multichannel chart recorder. The receiver output was sampled using the mercury jet commutator described by Bowles [1961], and an RC averaging time constant of 1 sec smoothed the sampled output of the recorder. The system was checked by recording random noise variations due to the signal from a noise diode generator fed in parallel to the RF inputs of the two receivers. The records obtained on the two channels were closely correlated. A Measurements Corp., Model 80 signal generator, containing a crystal oscillator control, was used to calibrate the receiver gains. The attenuator on the signal generator therefore served as the measure of relative power.

Our final result is that we find $\eta_r\eta_s=0.63\pm 0.05$. We hope to improve the accuracy of this result during subsequent moon passes through the beam.

2.4. τ —Transmitted Pulse Duration

The duration of the transmitted pulse is measured using a Tektronix 545 oscilloscope, observing the output of a diode sampler in the transmitter output transmission line. This measurement is estimated to be accurate to ± 2 percent.

2.5. P_t —Transmitted Power

The measurement of P_t is accomplished using a directional coupler built into a section of the 6 in. coaxial transmission line. This directional coupler, and associated bolometer measuring equipment, was built by P. A. Hudson at the NBS Radio Standards Laboratory in Boulder. He estimates the accuracy of this instrument, under our working conditions, to be ± 2 percent of the average power. Both power delivered to the transmission line, and power reflected from the transmission line are measured. During none of our tests was the reflected power more than about 0.3 percent of the power delivered to the line.

The pulse repetition frequency of the system was measured by comparing readings from three separate Tektronix 535 oscilloscopes. Normally we operated at a PRF of $49.5\text{ c/s}\pm 1$ percent.

The values of P_t given in table 1 are values measured with the bolometer, but reduced by the factor 0.82, to account for resistive losses in temporary transmission lines and ATR switch between the directional coupler and the antenna feed. From the fact that the temperature of the tungsten rods of the ATR never exceeded a value more than warm to the touch, we estimate that less than 2 percent of the indicated 4 kw of average transmitted power could have been dissipated in the ATR. Subsequent measurements will not suffer from this uncertainty due to a relocation of the directional coupler.

The absolute accuracy of the values of P_t , given in table 1, is therefore estimated to be about ± 4

percent. The internal accuracy of the measurements should be considerably better since the conditions of the measurement of P_t were not changed significantly during this series of measurements.

2.6. P_r —Received Power

The secondary standard of received power was a Measurements Corp. Model 80 signal generator with crystal oscillator, which had previously been calibrated using a micropotentiometer built at the NBS Radio Standards Laboratory. The accuracy of the measurement was ± 2.5 percent signal voltage, or ± 5 percent power, due mainly to the difficulty of making precise attenuator settings.

Routine calibrations of the receiver were made with a 5722 noise diode source constructed at NBS. The accuracy of the noise diode calibrations was assured by the fact that the noise bandwidth of the receiver was measured by comparing the noise diode input with the Model 80 signal generator input for the same deflection of the integrated receiver output. (See Bowles [1961] for details of the receiver "integrator" and display system.) The bandwidths obtained agreed, within ± 5 percent, with values estimated from the CW bandpass characteristics of the receivers.

The receiver IF output was square-law detected in a Ballantine Instruments Model 320 electronic voltmeter. Over the range of gain in use, the entire system from RF input to integrator display exhibited a response characteristic indistinguishable from proportionality to the input power. Since the scattered echoes have the characteristics of electrical noise, we preferred to use the noise diode generator for routine calibrations. While the Model 80 signal generator calibrations of the receiver exhibited the same power response characteristics, difficulties of using the Model 80 associated with slight power instability of the crystal oscillator precluded its use. In table 1 we list the *equivalent* noise diode current I_a in ma. Most calibrations were made using noise diode currents of 5.0 and 20.0 ma to establish the gain of the system. For this purpose a pushbutton Daven attenuator was used between the low noise RF amplifier and converter unit, and the main IF amplifier. By varying the attenuation in steps of 1 db, the noise diode deflection could be made to approximate the deflection of the incoherent scatter echo.

The internal resistance of the noise diode generator was 50 ohms. We calculated the value of P_a , the available power from the noise diode deliverable to a 50 ohm resistor of the receiver terminals, using the formula [Goldberg, 1948]

$$P_a=4.0\times 10^{-21}I_aB \quad (17)$$

where B is the receiver noise bandwidth expressed in cycles per second (the bandwidth of a receiver accepting an equal amount of noise but having a rectangular bandpass characteristic), and I_a is the noise diode current expressed in milliamperes.

At any height, R , then the value of the available receiver power from the antenna at the receiver terminals is $P_r = P_a$, corrected to correspond to the same integrator display deflection. We estimate that the absolute accuracy of this measurement was ± 10 percent power. The internal accuracy of the measurement, i.e., the variation from one measurement to the next, was about ± 5 percent.

2.7. N —Concentration of Free Electrons

We depend upon knowledge of the density of free electrons at the maximum of the F_2 layer based upon measurements of f_oF_2 . This information is measured using a conventional type C4 ionosonde, located right at the Lima Observatory. The observations of f_oF_2 are made within less than 5 min of the incoherent scatter measurements. Values of the penetration frequency of the ordinary trace can generally be made to an accuracy of ± 2 percent. Using the formula

$$N_{\max} = 1.24 \times 10^{10} (f_oF_2)^2 \text{ electrons per m}^3$$

with f_oF_2 expressed in Mc/s, we estimate the accuracy of this measurement to be ± 4 percent.

2.8. R_{\max} —Range to the F_2 Layer Maximum

Measurements of R_{\max} are based on scalings of the integrated A scope profile of incoherent scattered power. Figure 1 is an example of one of the A scope observations. Figure 2 is the electron density profile deduced from figure 1 by multiplying each value of P_r by R^2 . The value of R_{\max} is estimated from the electron density profile.

It might appear that the $500 \mu\text{sec} = \tau$ used in most of the measurements reported in table 1 would distort the profile of measured electron density. However, none of the observations have been made at times when the scale height at R_{\max} was smaller than the 75 km height resolution of the system. While slight distortion of the curve may be expected higher in the ionosphere, where the decay of P_r with height becomes abrupt, the distortion at R_{\max} is expected to be small. If anything we underestimate the value of P_r by perhaps 5 percent by not taking this effect into account. No correction has been made for this effect in table 1.

From the curve of $N(R)$, e.g., figure 2, it is possible to estimate the value of R_{\max} within ± 10 km. An additional difficulty is experienced in synchronizing the oscilloscope display to better than about ± 10 km. Much of the variation of accuracy from one measurement to the next due to this problem has been removed by using the positions of the individual points in the integrator display as a measure of R . Thus the fluctuations among the various measurements due to the difficulty of synchronization are largely removed by averaging over several measurements. We estimate the absolute accuracy of R_{\max} in most of the measurements to be ± 20 km. This gives an absolute percentage accuracy of R_{\max}^2 of about ± 12 percent. The internal accuracy of the measurement should be ± 6 percent.

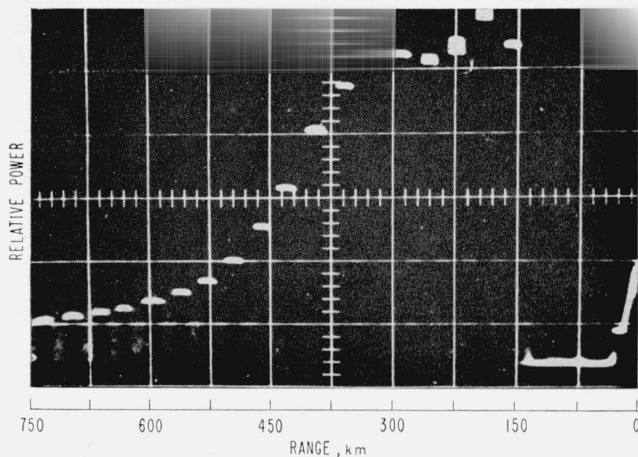


FIGURE 1. A 'scope photograph on 15 August 1961 at 0902 EST.

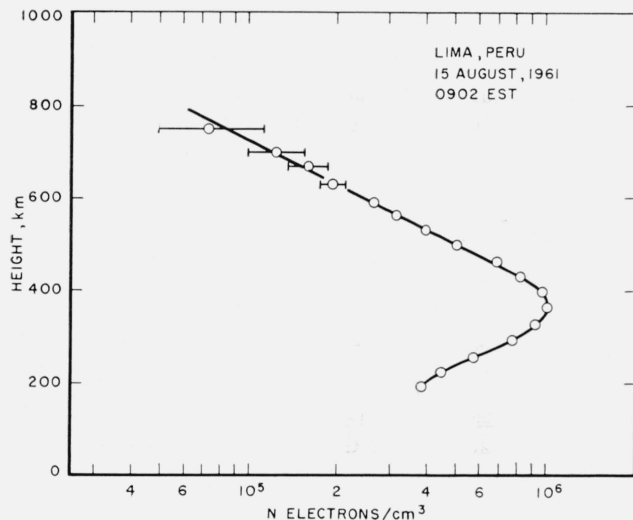


FIGURE 2. Electron density profile computed from figure 1.

2.9. Discussion of Accuracy of the Measurement

In table 2 we list each of the measured quantities next to its estimated error as given in the preceding paragraphs. We have every reason to believe that the statistical distributions of the errors for each of the measured values are approximately Gaussian, and mutually independent. Designating the individual error values as $\epsilon_1, \epsilon_2, \dots$, we estimate the probable range of error ϵ of the measured value of σ_m as $\epsilon = (\epsilon_1^2 + \epsilon_2^2 + \dots)^{1/2}$. The result of this calculation is that we are confident of the result of our measurement within ± 20 percent, i.e., ± 0.9 db. From similar considerations the internal accuracy of the measurement for intercomparison of results in table 1 would be ± 9 percent i.e., ± 0.45 db.

TABLE 2

Measured quantity	Estimated error $\pm 0/0$
ηA -----	10
$(\eta_r \eta_e)^2$ -----	2
P_i -----	4
P_r -----	10
N -----	4
$(R_{max})^2$ -----	12

2.10. Bandwidth Considerations

It will be noted in table 1 that we have employed receiver bandwidths of 2.54, 3.65, and 5.64 kc/s. All of these are larger than the bandwidth of approximately 1.8 kc/s corresponding to the 500 μ sec transmitted pulses normally employed. By direct scaling of the results of Pineo et al., [1960a and b] to our operating frequency of 49.92 Mc/s, we estimate that the width of the incoherent scatter spectrum from the F_2 layer should be on the order of 1,200 c/s. The received spectrum should be the convolution of this with the 1.8 kc/s transmitted spectrum. Thus we estimate that little or none of the echo power will be rejected by the receiver pass band.

This point was checked on several occasions when measurements of σ_m were made in rapid succession at two bandwidths. Consultation with table 1 will show that this estimate was correct. Recently we have made observations of the echo spectrum using a sweep frequency spectrum analyzer. The results are sufficiently accurate to show that the characteristic spectrum of the incoherent scatter during the day is essentially as given by Fejer [1961] for the case $T_e = T_i \cong 1500$ $^{\circ}$ K (± 500 $^{\circ}$ K), at the peak of the F_2 layer. During the day there is no evidence that the spectrum exhibits more than the very slight double peaking characteristic of $T_e = T_i$. Approximate spectra obtained during the sunrise period were about 50 percent wider than those obtained during the daytime, and exhibited a characteristic closely approximating Fejer's curve for $T_e/T_i = 2$.

2.11. Absorption

In so far as we are aware, ionospheric absorption of the radio waves is the only quantity not yet discussed which is likely to affect the result of our absolute measurement of σ_m . At our operating frequency of 49.92 Mc/s the ionospheric absorption in the daytime is thought to be on the order of $\frac{1}{2}$ db in the equatorial region [Little et al., 1956; Fredriksen and Dyce, 1960]. Unfortunately absolute values of this absorption have not been made in the equatorial belt. However the observations of Fredriksen and Dyce suggest that the absorption at night may at least occasionally be on the order of twice to three times as great as the daytime values.

We are left to presume that the bulk of the daytime absorption amounts to about 0.5 db (with a factor of 2 uncertainty) at 50 Mc/s and that most of this absorption occurs below the peak of the F_2 layer. We therefore assume that it would be correct to increase our measured values of σ_m by 1.0 db (or a factor of about 1.3) in the daytime to account for the double absorption on the round trip from transmitter to receiver. At midnight it may be correct to increase the observed values by 2 db (or a factor of about 1.6).

3. Observations of σ_m

Our observations of σ_m , made up to this time, have been restricted by the construction program at the Lima Observatory. We do not represent that the 23 individual observations thus far made constitute a complete study of the subject, and a comprehensive series of these observations is planned. Approximately half of the 23 observations were made during or just following the sunrise period when the ionization density in the F region was increasing rapidly, since the values of σ_m obtained during that period deviated considerably from values found during the remainder of the day. During the period of these observations the Galactic plane transited the beam in the evening hours. The resultant higher level of cosmic noise prevented successful evening observations during the present study.

We have already referred to table 1, in which the details of the several observations are given. The values of σ_m given in table 1 are also displayed in graphical form in figure 3a. No correction of ionospheric absorption has been made either in table 1 or in figure 3a.

As per eq (1), σ_m should be 4.99×10^{-29} m² under conditions of thermal equilibrium. Except during the sunrise period, ionospheric absorption can easily account for the somewhat lower values observed. In figure 3b, we give the values of one-way ionospheric absorption, in decibels, *required to correct* each observed value of σ_m to the theoretical value.

In figure 3b we have omitted values obtained during the sunrise period in view of the approximate spectrum result given at the end of section 2. Lacking an explicit expression for the expected value of σ_m as a function of T_e/T_i in Fejer's [1961] work, we have graphically integrated the spectra given in his figure 2. The result of this integration is shown in figure 4 which gives σ_m versus T_e/T_i . As may be seen by comparing figure 3 with figure 4, one would estimate that at sunrise in the F_2 region $T_e/T_i = 2$ which agrees with our spectrum estimate. From Fredriksen and Dyce [1960], we conclude that even at sunrise one would expect one way ionospheric absorption at the equator to be on the order of 0.5 db.

Thus far we have made daytime spectrum observations only in the height region from 300 to about 700 km. In that region there is no evidence of a significant change in the spectral characteristics in the very few observations we have to report until now.

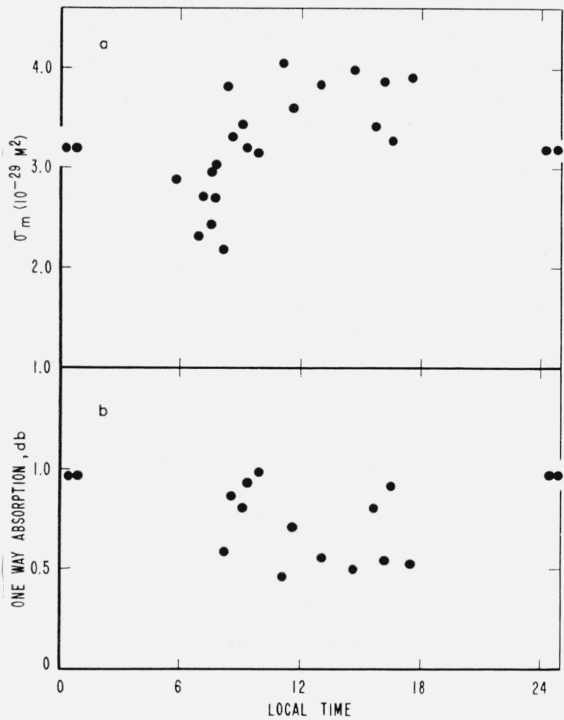


FIGURE 3. a. Values of σ_m computed for the scatter observations.
See table 1.
b. One way absorption required to make the observed values of σ_m agree with theory.

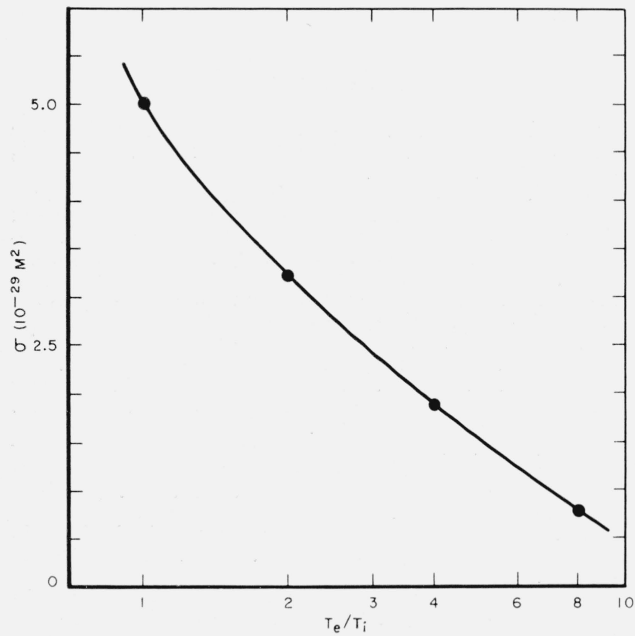


FIGURE 4. Dependence of σ_m on T_e/T_i .
(Adaptation of work by Fejer)

3.1. Spread-F

On several occasions during the hours between sunset and sunrise we have observed echoes at 50 Mc/s coinciding in time and height with spread-F echoes on the C4 sounder. For reasons given by Cohen and Bowles [1961], we believe that these are due to magnetic-field-aligned F region irregularities. We have observed strong echoes from spread-F on several occasions just prior to and during part of the sunrise period. The presence of these echoes of course prevented our making incoherent scatter observations simultaneously at least at these height ranges.

The advent of sunrise, and the gradual increase of ionization density in the F region, coincide with the gradual decay and disappearance of the spread-F echo. When the spread-F echo is intense it generally is broken into several discrete echoes, as illustrated by the A' scope photograph of figure 5, shown with its associated C4 record. After the spread-F has disappeared from the conventional ionogram, a

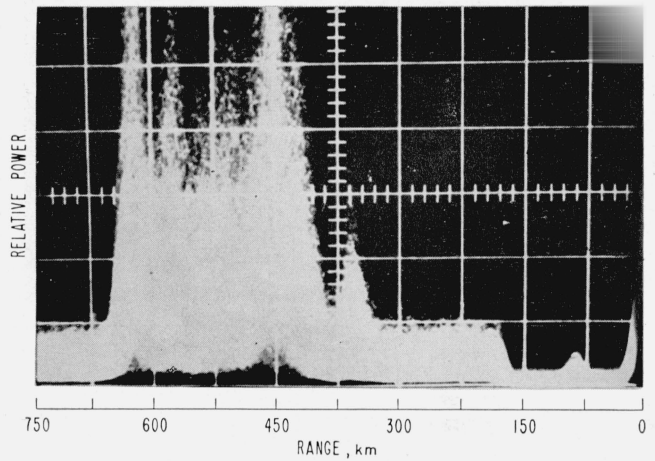


FIGURE 5a. Spread F on 15 August 1961 at 0559 EST— A' scope photograph—50 Mc/s.

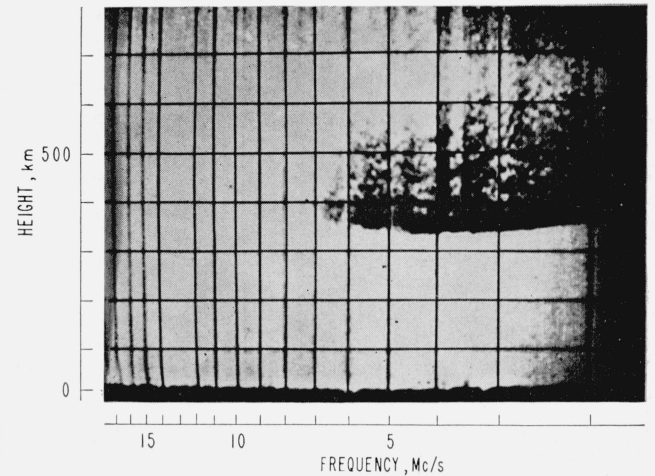


FIGURE 5b. Spread F on 15 August 1961 at 0559 EST— C_4 trace.

residual echo remains above the F layer maximum in the 50 Mc/s observations. This echo loses its discrete characteristic and blends into the smooth variation of echo intensity with height. This echo by its intensity would frequently lead one to interpret the scatter observations as indicating the presence of a G layer, above the F_2 layer, with $f_0G > f_0F_2$. If this were true we would expect to see the G layer trace on the conventional ionogram. Since we do not see such a trace on the ionogram, the residual echo, though spread smoothly over several hundred kilometers of height, must be interpreted as associated with the spread- F seen earlier. A typical A' scope display from the 50 Mc/s equipment is shown in figure 6. Thus far we have made no spectrum observation of the residual spread- F echo. All observations made thus far have been at an angle of propagation differing by about 3° from perpendicular to the earth's magnetic field lines.

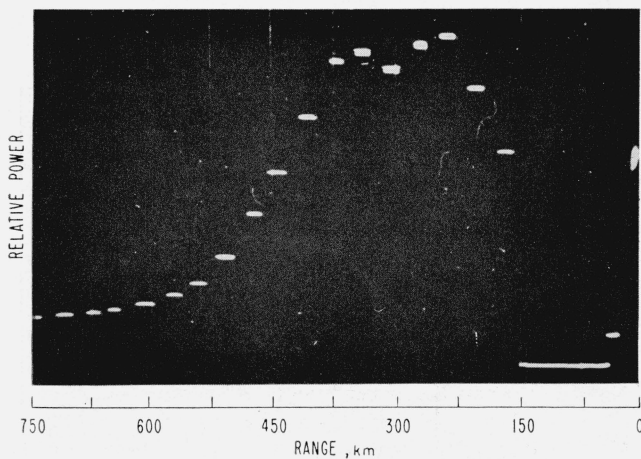


FIGURE 6. A' scope photograph (with integration) taken about one half hour after the obvious manifestations of spread- F , seen in figure 5, had disappeared.

It is obvious that under the conditions giving rise to the residual spread- F echo the computed value of the scatter cross section per free electron would be considerably in excess of the theoretical value given in eq (1). During periods when there is reason to suspect the presence of such echoes, the use of the incoherent scatter as a measure of the profile of electron density must be seriously impaired. Fortunately our observations indicated that these conditions are present only a small percentage of the time.

4. Conclusion

We conclude that in general the measured values of σ_m , the scattering cross section per free electron in "incoherent scatter" from the ionosphere, may be considered equal to the theoretical value $\sigma_m = 4.99 \times 10^{-29} \text{ m}^2$ during most of the day. During periods when it is reasonable to expect that thermal equilibrium may not exist, the measured values may depart from this ideal. At sunrise, when newly released electrons having kinetic energies considerably higher

than the average thermal energy of the ambient electrons may be expected to make up a significant percentage of the total, we find the observations suggest $T_e/T_i = 2$. Our results agree with the less accurate observations of Bowles [1961], made at 40.92 Mc/s at temperate latitude. They appear to agree reasonably well with the observations of Pineo et al. [1960a and b] at 440 Mc/s, although their interpretation of their results leads them to a contrary conclusion.

We conclude that within the height range of our present set of observations (200–1,000 km) the form of the electron density profile may be obtained by plotting $P_r R^2$ versus R , under most conditions encountered in the ionosphere. When it is known that $T_e \neq T_i$, spectrum observations can be used to correct the profile of P_r . Measurements presently available suggest that ignorance of T_e/T_i would introduce no more than a factor of 2 error at any point on the electron density profile within this height range. When spread- F is present, suggesting the possibility of a large departure from thermal equilibrium, the error would of course be larger.

We acknowledge with gratitude the help, encouragement, and active participation in our work of our many colleagues at the Instituto Geofísico del Perú, and at the National Bureau of Standards, notably R. Cohen. We have benefited from discussions with V. C. Pineo, J. A. Fejer, H. G. Booker, and V. R. Eshleman.

This work is supported jointly by the Government of the United States through the U.S. National Bureau of Standards and the U.S. Air Force, and by the Government of Perú through the Instituto Geofísico del Perú.

References

- Bowles, K. L., Observations of vertical incidence scatter from the ionosphere at 41 Mc/s, *Phys. Rev. Letters* **1**, 454–455 (Dec. 15, 1958).
- Bowles, K. L., Incoherent scattering by free electrons as a technique for studying the ionosphere and exosphere: Some observations and theoretical considerations, *J. Research NBS* **65D** (Radio Prop.), No. 1, 1–14 (January 1961).
- Buneman, O., Fluctuations in a multicomponent plasma, *J. Geophys. Research* **66**, 1978–1979 (1961).
- Cohen, R., and K. L. Bowles, On the nature of equatorial spread F , *J. Geophys. Research* **66**, 1081–1106 (1961).
- Dougherty, J. P., and D. T. Farley, A theory of incoherent scattering of radio waves by a plasma, *Proc. Roy. Soc. (London)* **259A**, 79–99 (1960).
- Farley, D. T., J. P. Dougherty, and D. W. Barron, A theory of incoherent scattering of radio waves by a plasma II scattering in a magnetic field, *Proc. Roy. Soc. (London)* **263A**, 238–258 (1961).
- Fejer, J. A., Scattering of radio waves by an ionized gas in thermal equilibrium, *Canadian J. Phys.* **38**, 1114–1133 (1960a).
- Fejer, J. A., Radio wave scattering by an ionized gas in thermal equilibrium, *J. Geophys. Research* **65**, 2635–2636 (1960b).
- Fejer, J. A., Scattering of radio waves from an ionized gas in thermal equilibrium in the presence of a uniform magnetic field, *Canadian J. Phys.* **39**, 716–740 (1961).

- Fredriksen, A., and R. B. Dyce, Ionospheric absorption investigations at Hawaii and Johnston Island, *J. Geophys. Research* **65**, 1177-1181 (1960).
- Goldberg, H., Some notes on noise figures, *Proc. IRE* **36**, 1205-1214 (1948).
- Gordon, W. E., Incoherent scattering of radio waves by free electrons with applications to space exploration by radar, *Proc. IRE* **46**, 1824-1829 (Nov. 1958).
- Gordon, W. E., and L. M. LaLonde, The design and capabilities of an ionospheric radar probe, *Trans. IRE* **AP9**, 17-22 (1961).
- Hagfors, T., Density fluctuations in a plasma in a magnetic field with applications to the ionosphere, *J. Geophys. Research* **66**, 1699-1712 (1961).
- Laaspere, T., On the effect of a magnetic field on the spectrum of incoherent scattering, *J. Geophys. Research* **65**, 3955-3959 (1960).
- Little, C. G., W. M. Rayton, and R. B. Roof, Review of ionospheric effects at VHF and UHF, *Proc. IRE* **44**, 992-1018 (1956).
- Lovell, B., and J. A. Clegg, *Radio Astronomy*, p. 135 (Chapman and Hall Ltd., London, 1952).
- Millman, G. H., A. J. Moceyunas, A. E. Sanders, and R. F. Wyrick, The effect of Faraday rotation on incoherent backscatter observations, *J. Geophys. Research* **66**, 1564-1568 (1961).
- Mills, B. Y., O. B. Slee, and E. R. Hill, A catalog of radio sources between declinations 10° N and 20° S, *Australian J. Phys.* **11**, 350-387 (1958).
- Pineo, V. C., L. G. Kraft, and H. W. Briscoe, Ionospheric backscatter observation at 440 Mc/s, *J. Geophys. Research* **65**, 1620-1621 (1960a).
- Pineo, V. C., L. G. Kraft, and H. W. Briscoe, Some characteristics of ionospheric backscatter observed at 440 Mc/s, *J. Geophys. Research* **65**, 2629-2633 (1960b).
- Pineo, V. C. and H. W. Briscoe, Discussion of incoherent backscatter power measurements at 440 Mc/s, *J. Geophys. Research* **66**, 3965-3966 (1961).
- Rayleigh, J. W. S., On the light from the sky, its polarization and color, *Phil. Mag. Series 4*, **1**, 107-120 (1871).
- Renau, J., Scattering of electromagnetic waves from a non-degenerate ionized gas, *J. Geophys. Research* **65**, 3631-3640 (1960).
- Renau, J., H. Camnitz, and W. Flood, The spectrum and the total intensity of electromagnetic waves scattered from an ionized gas in thermal equilibrium in the presence of a static quasi-uniform magnetic field, *J. Geophys. Research* **66**, 2703-2732 (1961).
- Richtmyer, F. K., E. H. Kennard, and T. Lauritsen, *Introduction to Modern Physics*, p. 351 (McGraw-Hill Book Co., Inc., New York, N.Y., 1955).
- Salpeter, E. E., Scattering of radio waves by electrons above the ionosphere, *J. Geophys. Research* **65**, 1851-1852 (1960a).
- Salpeter, E. E., Electron density fluctuations in a plasma, *Phys. Rev.* **120**, 1528-1535 (1960b).
- Salpeter, E. E., Effect of the magnetic field on ionospheric backscatter, *J. Geophys. Research* **65**, 982-984 (1961a).
- Salpeter, E. E., Plasma density fluctuations in a magnetic field, *Phys. Rev.* **122**, 1663-1674 (June 15, 1961b).
- Schelkunoff, S. A., and H. T. Friis, *Antennas, Theory and Practice* chs 1 and 5 (John Wiley and Sons, New York, 1952).
- Silver, S., *Microwave Antenna Theory and Design*, ch. 2 (McGraw-Hill Book Company, New York, 1949).
- VanZandt, T. E., and K. L. Bowles, Use of incoherent scatter technique to obtain ionospheric temperatures, *J. Geophys. Research* **65**, 2627-2628, (1960).

(Paper 66D4-203)